

The Atmosphere of Mars: A Comparison of Different Model Studies Based on Mariner IV Occultation Data

by

Gunnar Fjeldbo
Wencke C. Fjeldbo
Von R. Eshleman

N66 37214

FACILITY FORM 602

(ACCESSION NUMBER) 24

(PAGES) CR-78134

(NASA CR OR TMX OR AD NUMBER)

(THRU) 1

(CODE) 30

(CATEGORY)

June 1966

GPO PRICE \$ _____

CFSTI PRICE(S) \$ _____

Hard copy (HC) \$1.00

Microfiche (MF) 150

ff 653 July 65

Scientific Report No. 16

Prepared under
National Aeronautics and Space Administration
Grant NsG-377
and

Scientific Report No. 3

Prepared under
National Aeronautics and Space Administration
Contract NGR-05-020-065

RADIOSCIENCE LABORATORY

STANFORD ELECTRONICS LABORATORIES

STANFORD UNIVERSITY • STANFORD, CALIFORNIA



THE ATMOSPHERE OF MARS: A COMPARISON OF DIFFERENT
MODEL STUDIES BASED ON MARINER IV OCCULTATION DATA

by

Gunnar Fjeldbo
Wencke C. Fjeldbo
Von R. Eshleman

June 1966

Reproduction in whole or in part
is permitted for any purpose of
the United States Government.

Scientific Report No. 16

Prepared under
National Aeronautics and Space Administration
Grant NsG-377

Scientific Report No. 3

Prepared under
National Aeronautics and Space Administration
Contract NGR-05-020-065

Radioscience Laboratory
Stanford Electronics Laboratory
Stanford University Stanford, California

ABSTRACT

Three classes of models for the atmosphere of Mars are compared. They are called F_2 , F_1 , and E models, by analogy with the formation of these ionized layers in the earth's upper atmosphere. In the F_2 models, CO_2 is dissociated by solar ultraviolet radiation at approximately 70 km altitude, and atomic oxygen predominates above 80 km when diffusive separation is assumed to start near the dissociated region. The principal ion in the main daytime ionospheric layer measured by Mariner IV would thus be O^+ , and the topside of the layer would be isothermal at approximately 90 °K, to correspond with the observed constant plasma scale height of about 26 km. The mesopause temperature minimum would be at or below the freezing point of CO_2 , and dry ice particles would be expected to form. In the F_1 models, molecular constituents predominate in the upper atmosphere to an altitude of approximately 225 km, and molecular ions (CO_2^+ , CO^+ , or O_2^+) formed by solar ultraviolet radiation and various chemical reactions would make up the ionospheric layers. The temperature in the isothermal height region (125 to approximately 225 km) would thus be between about 150 and 250 °K, depending on constituents. In the E model proposed by Chamberlain and McElroy, the main ionization layer is assumed to be formed by solar X-rays in a mixed upper atmosphere. Temperature gradients would be required above the ionization peak to conduct energy down from regions heated by solar ultraviolet radiation, with the temperature reaching 400 °K at about 250 km altitude. The mass density in the upper atmosphere for the E model would be more than two orders of magnitude larger than for the F_1 models, and about 10^4 times the mass density at the same altitudes in the F_2 models. We conclude that the F_2 models fit theory and observation best, and identify the reaction which is critical in defining a particular F_2 model. However, an F_1 model might result if photodissociation and diffusive separation are markedly less than would be expected by analogy with the earth's upper atmosphere. The E model appears very unlikely to us. It was introduced by Chamberlain and McElroy primarily because their temperature

computations are not consistent with the temperature profiles of F_2 and F_1 models such as discussed here. However our heat-budget computations indicate markedly lower temperatures and temperature gradients for the atmospheric region probed by Mariner IV, and we conclude that neither the F_2 nor F_1 models can be ruled out from such admittedly incomplete physical analyses. Also, the temperature profile for the E model is not compatible with the measured plasma scale height unless very unlikely and arbitrary assumptions are made about the change with height of the values of the effective recombination coefficient and the average ion mass.

TABLE OF CONTENTS

	<u>Page</u>
I. GENERAL DISCUSSION	1
II. THE HEAT BUDGET OF THE UPPER ATMOSPHERE	9
III. EMERSION MEASUREMENTS	15
IV. CONCLUDING REMARKS	17
REFERENCES AND NOTES	19

ILLUSTRATIONS

Figure

1 Number density vs altitude for three different atmospheric models	2
2 Temperature vs altitude for three different atmospheric models	3
3 Two-way ionospheric phase path vs altitude above the limb. .	7
4 Temperature vs distance below the thermopause for a sample of theoretical heat balance calculations discussed in the text	11

I. GENERAL DISCUSSION

The observational evidence provided by Mariner IV (1) has led to three markedly different types of models for the Martian atmosphere. They differ in particular in explaining the characteristics of the main ionization layer observed in the atmosphere of Mars over Electris, near 50° S latitude and 177° E longitude at 1300 local time in late winter. By analogy with the formation of ionization layers in the earth's upper atmosphere, we shall denote these three classes of models as F_2 , F_1 , and E.

The F_2 or Bradbury models rest on the assumption that the observed ionization peak results from a rapid upward decrease of the ion recombination loss coefficient, together with downward plasma diffusion. In the F_2 models, the electron density peak is above the region where most of the electron production and recombination occur.

The F_1 and E models are based on the assumption that the observed ionization profile is a Chapman layer where the peak coincides with the electron production peak caused by solar UV and X-rays, respectively.

The interpretation of the Mariner data in terms of F_2 and F_1 models was first suggested by the radio occultation team (2, 3) and later expanded upon by Fjeldbo et al (4). In each case, the F_2 explanation was favored. Number density and temperature profiles for these models are shown in Figs. 1 and 2. A different F_2 model has been proposed by Johnson (5), and discussions relative to other F_1 models have been given by Donahue (6) and by Smith and Beutler (7). Chamberlain and McElroy (8) have offered an E model, and the number density and temperature profiles for their model are also shown in Figs. 1 and 2. While rather particular F_2 , F_1 , and E models are shown in the figures and discussed below, most of the arguments presented here are applicable to a general comparison of these three classes of models.

Below about 30km altitude, there is not much latitude in determining the neutral number density and temperature profiles from the measured refractivity since the atmosphere must consist almost entirely of CO_2 (1). At ionospheric heights, the interpretation of the radio occultation data appears to be considerably more ambiguous, with proposed neutral

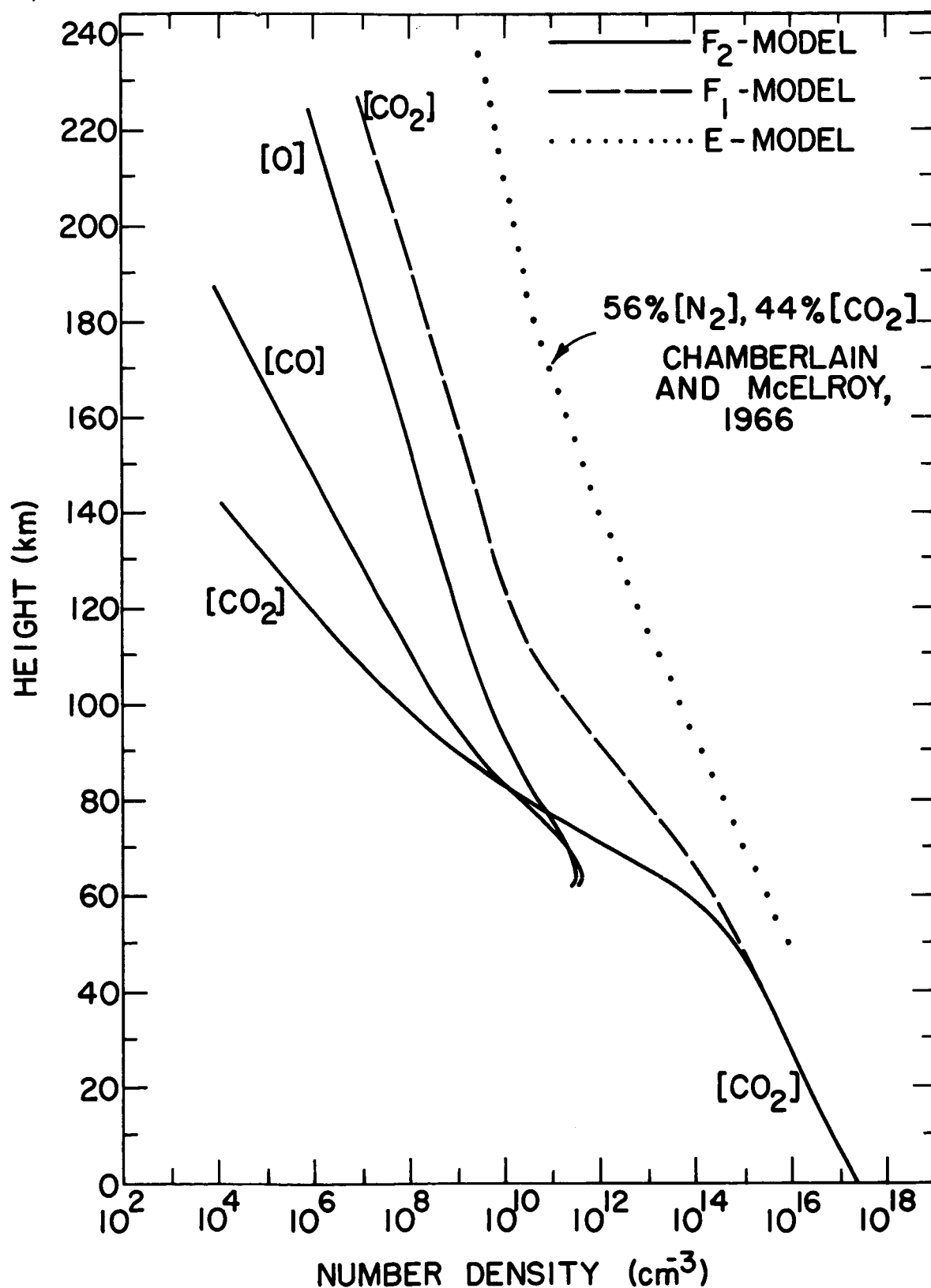


FIG. 1. NUMBER DENSITY VS. ALTITUDE FOR THREE DIFFERENT ATMOSPHERIC MODELS. The F₂ and F₁ models apply to the location and time of immersion into occultation. The E model was taken from Ref. 8.

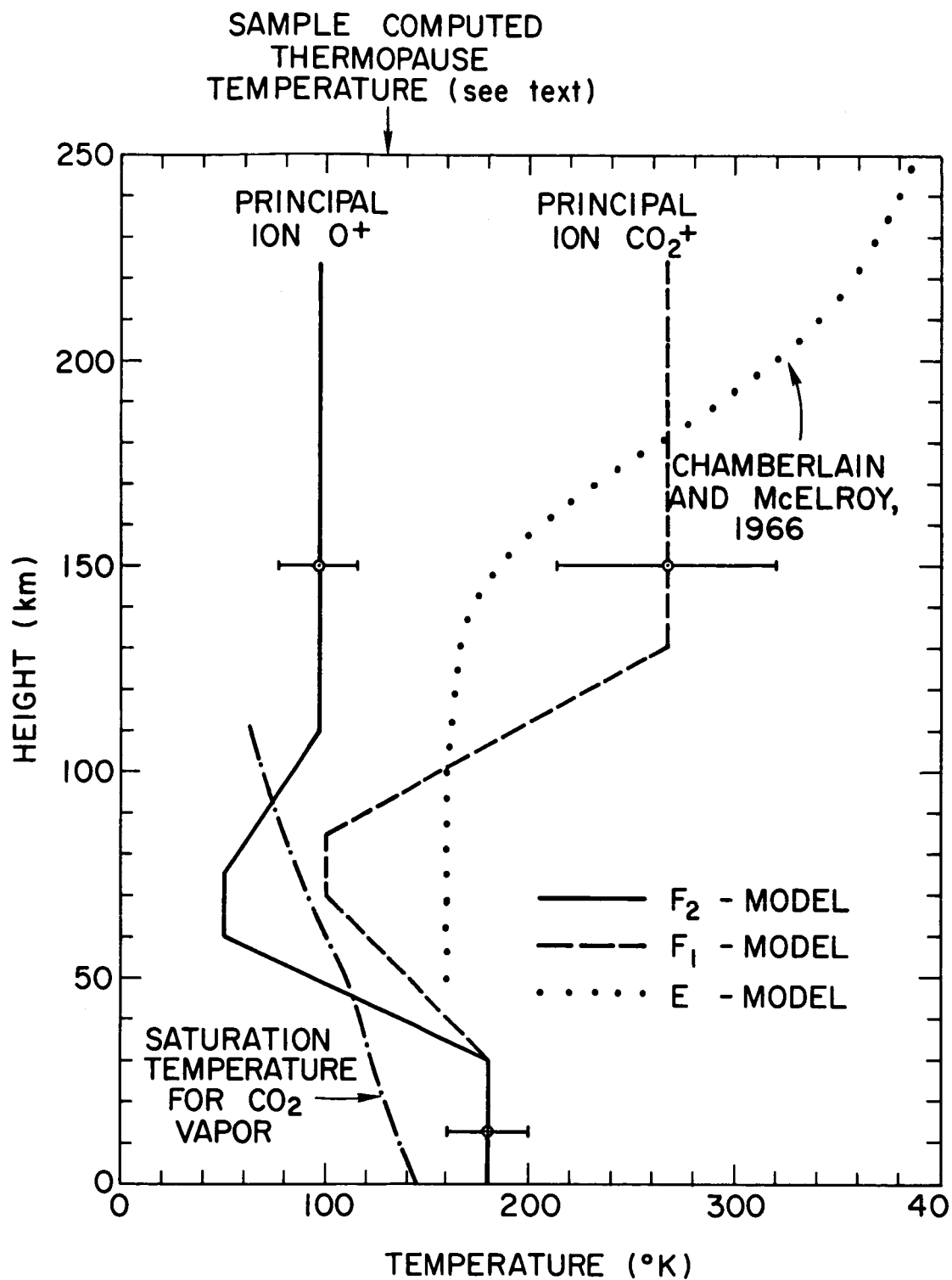


FIG. 2. TEMPERATURE VS. ALTITUDE FOR THREE DIFFERENT ATMOSPHERIC MODELS. The F_2 and F_1 models apply to the location and time of immersion into occultation. The E model was taken from Ref. 8.

number densities differing by factors up to 10^4 and suggested upper atmospheric temperatures varying from below 100 to more than 400 °K.

The full drawn curves of Figs. 1 and 2 apply to an F_2 model. In this model (3, 4) carbon dioxide is dissociated into atomic oxygen and carbon monoxide at about 70 km altitude. Above the dissociation region O, CO, and CO_2 are assumed to be in diffusive equilibrium so that the lightest constituent (O) predominates in the upper atmosphere. At the ionization peak (120 km altitude), the atomic oxygen density was determined by equating the photo ionization rate and the rate of downward plasma diffusion. The CO_2 density at this altitude was estimated by equating the rates of diffusion and recombination loss of electrons. The limiting recombination loss mechanism at the ionization peak used for this model is $O^+ + CO_2 \rightarrow O_2^+ + CO$, with a rate coefficient of 10^{-9} cm³/sec (3, 4).

Below the dissociation region, there might be layers of O_2 and O_3 (9). However, the chemical reaction rates are poorly known and the extent of mixing can only be estimated based on analogies with the earth's atmosphere; thus, the actual O_2 and O_3 densities are uncertain.

Above the ionization peak the atmospheric temperature for the F_2 model was determined from the observed plasma scale height assuming thermal equilibrium between the plasma components and the neutral gas. (The preliminary work (1) indicated a plasma scale height of about 20 to 25 km, while our later and more complete analysis gives 23 to 29 km. This spread is mainly due to variations in data taken at different tracking stations.)

Between approximately 30 and 100 km altitude above Electris, the refractivity was too low to be detected. However, one can utilize the temperature and density of CO_2 above and below to determine the average temperature for this intermediate region (4). Based on the theoretical heat balance computations discussed below, we put the mesopause temperature minimum at an altitude corresponding to a density level of about 10^{13} cm⁻³.

The F_2 temperature profile shown in Fig. 2 dips below the saturation temperature for CO_2 vapor. It is well known that supercooling of H_2O droplets takes place in our own atmosphere and an analogous situation might conceivably exist on Mars with regard to CO_2 . The main difference would be that, since the pressure is lower than the triple point, CO_2

remains in the gas phase rather than in the liquid phase. If, on the other hand, the sublimation time were shorter than the diffusion time in this region of the atmosphere, one would anticipate the formation of CO_2 particles so that the temperature profile might follow approximately the saturation temperature for CO_2 vapor (4). This effect might help explain some of the haze and particle layers observed with earth-based telescopes and with the Mariner IV TV camera, and perhaps also why pressure estimates based on optical scattering from the atmosphere of Mars gave a surface pressure approximately one order of magnitude larger than the values obtained from the occultation experiment, and the more recent spectroscopic observations.

The low temperatures required for the F_2 model of Figs. 1 and 2, in the atmospheric region between 30 and 100 km altitude, are a result of the high value measured for the rate coefficient for the charge rearrangement reaction between O^+ and CO_2 (4). However, there are also other considerations that suggest a cold intermediate region in the Martian atmosphere. Ohring has, for instance, made radiative transfer computations for the lower atmosphere and obtained stratospheric temperatures below the saturation temperature for CO_2 vapor (10). Similarly, earlier heat balance calculations for the upper atmosphere, reported by Chamberlain, gave a mesopause temperature of 76 °K (11). However, Chamberlain and McElroy (8) have objected to interpreting the observed ionization peak as an F_2 region primarily on the grounds that their theoretical estimates yield a thermopause temperature at least 4 times larger than the approximately 100 °K required for the F_2 model. (On the other hand, see the results and discussion below of other temperature computations.) Instead they suggest that the ionization peak should be interpreted as an E region produced by solar X-rays. The number density and temperature profiles for their model are shown by the dotted curves in Figs. 1 and 2.

To avoid the formation of an F_2 ionization peak, Chamberlain and McElroy assume that the upper atmosphere is mixed and that CO_2^+ is the predominant ion in the upper regions of the observed layer. For comparison, one might note that the earth's atmosphere is mixed only up to a density level of about 10^{12} to 10^{13} cm^{-3} , which occurs well below the F_2 and F_1 regions.

The absence of an F_1 ionization peak at about 200 km altitude in Chamberlain and McElroy's model requires the effective recombination coefficient to be larger at this altitude than in the E region below, while in the earth's atmosphere it decreases with altitude. In their Martian F_1 region the electron production rate and electron number density are of the order of $10^3 \text{ cm}^{-3} \text{ sec}^{-1}$ and 10^4 cm^{-3} , respectively. Thus, an effective recombination coefficient of about $10^{-5} \text{ cm}^3/\text{sec}$ would be necessary in order to account for the low electron density at this altitude. This value is 3 to 4 orders of magnitude greater than the effective recombination coefficient at corresponding density levels in the earth's atmosphere, and is 2 to 3 orders of magnitude larger than the central values given by Nawrocki and Papa (12) for dissociative recombination of CO_2^+ .

However, our major objection to an E region hypothesis is that it is difficult to make it compatible with the constant plasma scale height observed above the ionization peak. The measured two-way phase path data can be presented in such a way as to compare it directly with assumed scale heights, for a spherically symmetrical ionosphere. This has been done in Fig. 3, where it is seen that the plasma scale height is very nearly constant from just above the peak, at 120 km, to an altitude of 200 and perhaps even to 250 km, or over a height range of 3 to 5 plasma scale heights. Over this same height range, Chamberlain and McElroy suggest an increase in temperature by a factor of about 2.5. In order to maintain a constant plasma scale height in their model it would be necessary for the average ion mass to increase with altitude. With a constant recombination coefficient within the F_1 region, the ion mass would need to be approximately 55 and 65 at 200 and 220 km altitude, respectively, for a mean plasma scale height of 26 km.

If the upper atmosphere of Mars consists primarily of molecular constituents (such as CO_2 , CO, or O_2), the ionization peak might be produced by solar UV flux. This third alternative, denoted as the F_1 model, is also indicated in Figs. 1 and 2, assuming 100% CO_2 . In this model, the ionization peak occurs at a neutral density of about 10^{10} cm^{-3} where the slant optical depth in the ultraviolet part of the spectrum is unity.

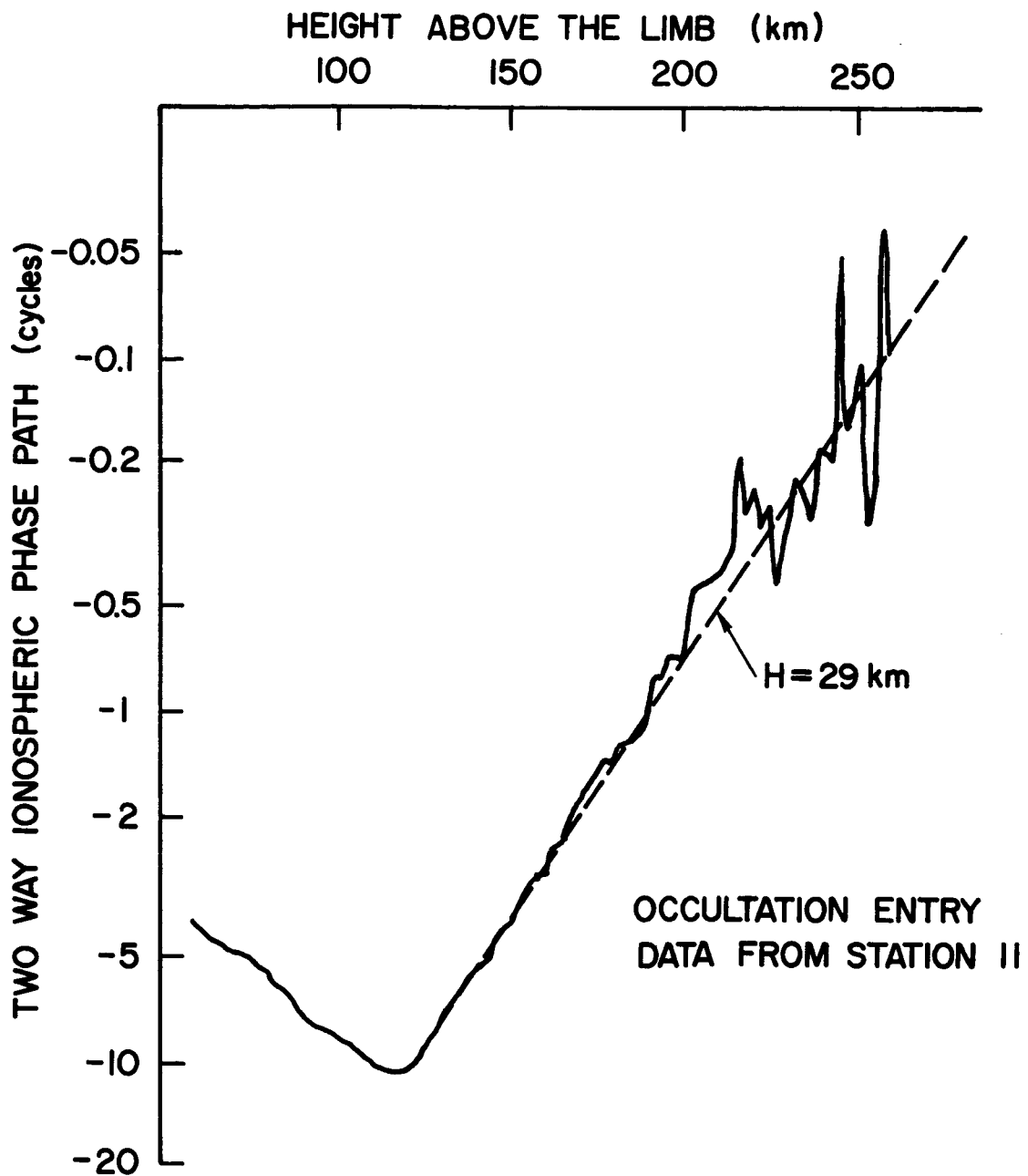


FIG. 3. TWO-WAY IONOSPHERIC PHASE PATH VS. ALTITUDE ABOVE THE LIMB.
 The full drawn curve represents station 11 data. The stippled curve corresponds to a theoretical model ionosphere with a topside plasma scale height of 29 km.

Both the E and F_1 hypotheses discussed here require mixing or negligible dissociation of CO_2 in order to avoid the preponderance of atomic oxygen in the region where the data show a constant plasma scale height. This is one of the reasons we favor the F_2 model (3, 4). Comparing only the F_1 and E models, we suggest that the F_1 is more attractive because:

- (1) No appreciable temperature gradients are expected on the topside of the F_1 peak since most of the solar flux is absorbed at lower altitudes. Thus, the topside plasma scale height would be constant without making any improbable assumptions about the altitude variations of the ion mass and the recombination coefficient.
- (2) In the F_1 region of the F_1 model, the recombination coefficient would need to be about $10^{-7} \text{ cm}^3/\text{sec}$ as compared with $10^{-5} \text{ cm}^3/\text{sec}$ in the F_1 region of the E model. This lower value is in better agreement with the value expected for dissociative recombination of CO_2^+ (12).

II. THE HEAT BUDGET OF THE UPPER ATMOSPHERE

In order to understand the physical reasons for the small plasma scale height and to help resolve the ambiguities in the interpretation of the occultation data, we have studied the heat budget of the Martian thermosphere. Many similar studies have been conducted in the past both for the earth and for the planets (11, 13), and some of these investigations have provided a very useful foundation for our work.

In this report, we shall restrict ourselves to a discussion of the thermal structure that prevailed in the ionospheric region probed by the telemetry link during immersion. Following earlier studies (11, 13), we neglect convective and advective transport of heat together with the effects of temperature transients. The heat balance equation can then be written:

$$\frac{\partial}{\partial h} \left(-K \frac{\partial T}{\partial h} \right) = \sum_i \sum_{\lambda} \epsilon_{\lambda} \sigma_{i\lambda} \frac{1}{2} I_{o\lambda} e^{-\tau_{\lambda}} n_i - \sum_i R_i \quad (1)$$

where

T = temperature

h = altitude

K = thermal conductivity

ϵ_{λ} = fraction of absorbed solar flux converted to local heat

$\sigma_{i\lambda}$ = absorption cross section for the i -th constituent at wavelength λ

$I_{o\lambda}$ = solar flux at the top of the atmosphere

$\tau_{\lambda} = \int_h^{\infty} \sum_i \sigma_{i\lambda} n_i \sec \chi \, dh$; optical depth

χ = solar zenith angle at noon

n_i = number density of i -th constituent

R_i = power loss by radiation from i -th constituent.

Equation (1) expresses that in a unit volume, the divergence of the conducted heat flux is equal to the input heat power associated with absorption of solar flux, less what is lost through infrared radiation.

The factor " $1/2$ " in front of the solar flux term takes into account, in an approximate way, the fact that the sun only heats the thermosphere for about 12 out of 24 hours, while the radiative cooling goes on also during the night. The temperatures obtained in this manner represent approximately a 24 hour average profile.

In the radiative loss terms (R_1), we have included emission in the CO_2 vibrational bands at $15\ \mu$, the rotational bands of CO , and the $62\ \mu$ band of the ground state of O . The effect of the finite atmospheric optical depth in these bands was also included.

The heat balance calculations delineated here do not apply below the level of vibrational relaxation which, for the F_2 and F_1 models of Figs. 1 and 2, occurs at approximately 30 km altitude. Below this region, the thermal structure is most likely controlled by radiative transfer and convection.

The solar zenith angle enters into Eq. (1) and causes the thermopause temperature to decrease with increasing solar latitude. This effect is not obvious in the earth's thermosphere, which is one indication that the mathematical model represented by Eq. (1) is oversimplified. It should also be pointed out that most of the parameters that enter into the solution of Eq. (1) are poorly known and this introduces additional uncertainties.

The following technique was used in solving the heat balance equation with respect to the temperature profile: the atmosphere was divided into stratified layers, and the boundary conditions at the thermopause were chosen based on the densities and temperatures given in Figs. 1 and 2, respectively. Proceeding downward from the thermopause, the temperature and neutral densities were computed in an iterative manner for each layer. The results of several such computations carried out for different thermopause temperatures are shown in Fig. 4. The number densities at the thermopause were taken from the F_2 model shown in Fig. 1. (It is not critical at which altitude the thermopause boundary is selected, as long as it is well above the F_1 region where the solar UV flux is absorbed.) With a boundary condition for the temperature profile of about 100°K at the thermopause, the atmosphere is seen to be too cold to conduct the heat flux downward to regions where it may be radiated away. A 200°K

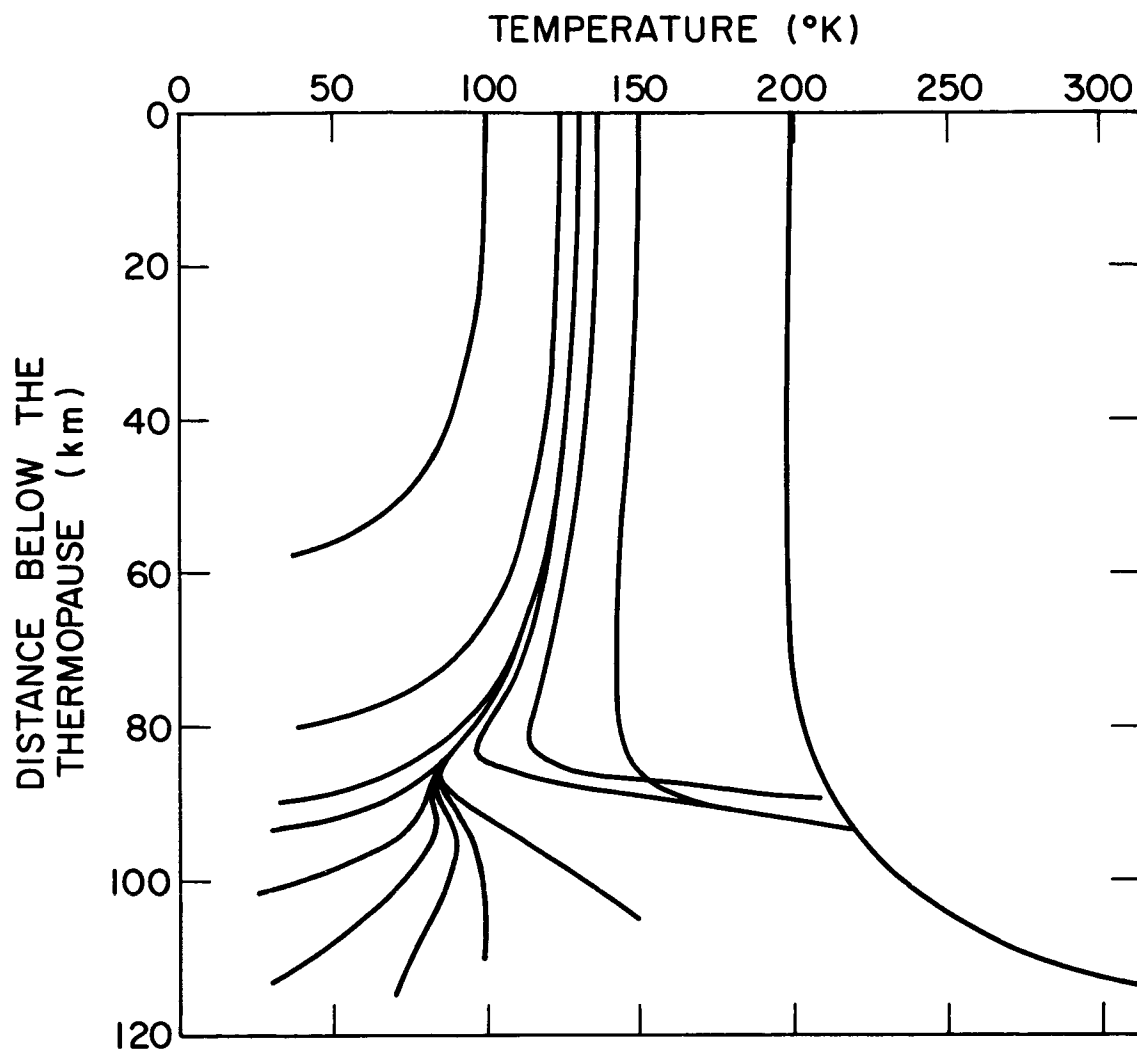


FIG. 4. TEMPERATURE VS. DISTANCE BELOW THE THERMOPAUSE FOR A SAMPLE OF THEORETICAL HEAT BALANCE CALCULATIONS DISCUSSED IN THE TEXT. The density at the mesopause, which is the altitude of minimum temperature near the base of the thermosphere, is about 10^{13} cm^{-3} .

temperature at the thermopause is, on the other hand, too high, and would require a large heat flux from below in order to replace what is lost through radiation. However, a thermopause temperature of about 130 °K gave a reasonable temperature profile for this sample computation. The temperatures in the mesosphere are seen to be very sensitive to changes in the boundary conditions at the thermopause. However, the important point to be noted here is not the actual shape of the profile in the mesosphere (since there are many complex processes affecting the temperature in this region), but the fact that these calculations yield a thermopause temperature that is between the approximately 100 °K required for the F_2 model and the 250 °K required for the F_1 model.

The temperature calculations described here were repeated for several different sets of input parameters (photo absorption cross sections, solar flux, efficiency of heating, etc.) and boundary densities at the top of the thermosphere. For instance, in some of these calculations, the upper atmosphere was assumed to consist of 100% CO_2 , which corresponds to the F_1 model of Figs. 1 and 2. This assumption gave a higher thermopause temperature than shown in Fig. 4 because the conductivity of CO_2 is lower than for O and also because there is no CO in the F_1 model that can help radiate the heat away. However, for all of these computations, the thermopause temperature over Electriss came out between 130 and 280 °K. Thus, the conclusion remains the same (14).

With some convection and perhaps radiation by constituents other than CO_2 , CO, and O, the temperature might presumably be even lower than the 130 °K shown in Fig. 4, and thus be in agreement with the F_2 model. However, if the plasma temperature were higher than the neutral gas temperature during the measurement, the F_1 model of Figs. 1 and 2 might be in best agreement with these estimates.

When we keep in mind the simplifications used in these temperature studies, and the number of uncertain parameters that enter into the problem, it is, in our opinion, not possible to reject either the F_2 or the F_1 model on the basis of heat-balance estimates. On this point, our work differs markedly from the results of Chamberlain and McElroy, who claim that the temperature on top of the thermosphere must be at least 400 °K (8). There are several reasons for this large disagreement:

- (1) Our calculations were made using a solar zenith angle (χ) of 67° , which applies to conditions where the Martian ionosphere was actually probed. Chamberlain and McElroy used $\chi = 60^\circ$.
- (2) Radiative cooling is more efficient in the lower thermosphere of our models since they have a higher abundance of CO_2 (and also more CO in the case of the F_2 model) than Chamberlain and McElroy's model, which has 56% N_2 and 44% CO_2 . Such a large percentage of N_2 seems unlikely in view of the small scale height (9km) measured in the lower neutral atmosphere over Electris because it might require that CO_2 be supersaturated in this region. It also gives rise to poor agreement between the surface pressures obtained from the occultation measurements and the spectroscopic studies (1, 4).
- (3) The conductivity for atomic oxygen is between 2 and 3 times greater than for a mixture of CO_2 and N_2 under equal thermal conditions, and this also contributes to the difference in the thermopause temperature for the F_2 and E models of Fig. 2.
- (4) In the sample calculations shown in Fig. 4, we used lower values for the quiet sunspot minimum solar flux than employed by Chamberlain and McElroy, based on tabulations given by Johnson (15).

The temperature calculations reported here show that the small top-side plasma scale height can be explained adequately with either the F_2 or the F_1 models. While our results are quite different from those of Chamberlain and McElroy, they do not preclude an E model with a lower high latitude thermopause temperature than was used by these authors. On other grounds, however, the E region interpretation appears to be the least plausible of these three alternatives, as discussed above.

Smith and Beutler (7) have recently computed a temperature profile for the subsolar region of Mars at sunspot maximum. They assume that O , CO , and CO_2 are in diffusive equilibrium in the upper atmosphere and obtain a thermopause temperature of approximately 400°K . While this is the same number as obtained by Chamberlain and McElroy, there is actually a large discrepancy since their computations were for sunspot minimum. The temperature results of Smith and Beutler are in fact in very good agreement with the sample computations shown in Fig. 4, since a simple

analogy with the earth's upper atmosphere suggests that the thermopause temperatures at sunspot maximum and minimum should differ by more than a factor of two. The remaining difference would presumably be explained by the latitude effect.

Smith and Beutler also attempt to explain the small plasma scale height observed by Mariner IV. They suggest that the observed ionization peak is an F_1 -type layer consisting predominantly of O_2^+ and with a temperature of 170 °K corresponding to a 25 km plasma scale height. However, this value for the temperature does not necessarily follow from the theory for such a layer. The O_2^+ ions are presumably produced mainly by photoionization of O followed by a charge rearrangement reaction with CO_2 ($O^+ + CO_2 \rightarrow O_2^+ + CO$). If so, the plasma scale height should be twice the scale height of the atomic oxygen profile in the region above the F_1 peak where ambipolar diffusion is negligible. Thus, in this region, a 25 km plasma scale height would still have to be interpreted in terms of an 85 °K topside temperature. The same is true at greater altitudes where the lifetime of O^+ becomes greater than that of O_2^+ .

Donahue (6) has also suggested that the main ionospheric layer observed on Mars is an F_1 region with O_2^+ being the principal ion. However, his atmospheric temperature profile, which is constant equal to about 160 °K below 150 km altitude, also appears to be inconsistent with the observed plasma scale height for similar reasons.

Another approach toward explaining the small plasma scale height has been attempted by Gross et al (16). They assume that O^+ is the principal ion on the topside but introduce temperature gradients in this region in order to avoid the low temperatures. However, in order to explain the constant scale height, this approach would require a temperature gradient which is increasing exponentially with altitude. Gross et al's temperature profiles do not exhibit this property in the altitude range of interest, and additional assumptions, such as a recombination coefficient that is increasing with altitude, would seem necessary in order to explain the observations.

III. EMERSION MEASUREMENTS

The number densities and temperatures of the F_2 and F_1 models of Figs. 1 and 2 were derived from the immersion data obtained over Electris, which is a bright area in the southern hemisphere of Mars. Measurements were also made during emersion from occultation, which occurred over Mare Acidalium near 60° N latitude, 36° W longitude, and about 2340 local time in late summer. The emersion data have been analyzed independently by the Jet Propulsion Laboratory and Stanford University members of the occultation experiment team. Our preliminary values for atmospheric pressure, temperature, and temperature lapse rate near the surface at Mare Acidalium are about 8.5 mb, 250° K, and 2.5° K/km, respectively, assuming 100% CO_2 . The tropopause was located at approximately 17 km altitude. These values are in good agreement with the emersion results of Kliore et al (17), and should be compared with 4.9 mb, 180° K, and zero lapse rate for the atmosphere over Electris (50° S, 177° E, 1300 local time, late winter) (1). The emersion values are considerably less certain than the immersion results because the spacecraft transmitter changed its frequency and mode of operation in the middle of the emersion measurements (1), and this causes problems in the interpretation of the data. Even so, it is difficult to avoid the conclusion that the surface pressure over Mare Acidalium was at least 50% greater than over Electris. Calculations of the radii of the two occulting features (measured from the Martian center of mass) have also been made, and we find that the radius at Electris (~ 3384 km) is approximately 4 km larger than the radius at Mare Acidalium. These calculations were based on the "best trajectory" determined by the orbit determination group of the Jet Propulsion Laboratory, a timing correction supplied by D. L. Cain of JPL, and the limb diffraction effects observed during signal extinction and commencement. The results agree closely with those of Kliore et al (17), who suggest a 5 km difference, a value of 3384 km at immersion, and possible errors in the radii of ± 3 km at immersion and ± 4 km at emersion.

These tentative results lead to several interesting and important implications. The differences in pressure and radius both suggest that the Martian maria may be lowlands and the bright area highlands. This

question is of considerable interest with regard to future instrument landings on Mars, both from scientific and engineering considerations. However, local terrain features at the occultation points, greater oblateness than a gravitational equipotential surface, and atmospheric circulation patterns might also contribute to the observed differences. The low daytime temperature in the lower atmosphere over Electris tends to support the carbon dioxide polar-cap theory which has been vigorously revived by Leighton and Murray (18). On the other hand, the relatively high temperature obtained at 60° N latitude suggests that the residual late summer polar cap is not likely to be dry ice since the nighttime atmospheric temperature was some 100 °K above the saturation temperature for CO₂ vapor, and the latitude separation was less than 30°. We are led to the preliminary suggestion that the winter polar cap may be predominantly dry ice, while the bottom part of the thicker central region (19), some of which persists through the summer, may be largely water ice.

The nighttime ionosphere over Mare Acidalium apparently had a density lower than about 5×10^3 electrons per cm³ (1). This upper limit to the electron number density does not affect any of the models shown in Figs. 1 and 2, since they all have short enough time constants (actually less than half an hour at the electron density peak) to account for a very low nighttime ionization level.

IV. CONCLUDING REMARKS

While theoretical atmospheric models based on analogies with any one of the ionized regions in the earth's upper atmosphere presumably can be tailored to fit the main ionization layer detected on Mars, we favor models of the F_2 type because they seem to account for the observed ionization profile in the most straightforward way. However, we may have overestimated the degree of photodissociation and diffusive separation--estimates which to a large extent are based on analogies with the earth's atmosphere. If so, the ionization peak should be identified as an F_1 region, i.e., a Chapman layer produced by solar ultraviolet flux (2, 3, 4). We suggest that model atmospheres based on parallelism between the Martian ionization peak and the terrestrial E (and also D) regions should be rejected since these models are inconsistent with the topside plasma scale height unless rather unlikely assumptions are made about the values and changes with height of the average ion mass and the recombination coefficient.

Arguments based on simplified temperature computations have been used to question the validity of F_2 models, and to support an E model. However, thermopause temperatures for the F_2 and F_1 models bracket temperatures derived from our similar computations of the heat budget in the upper atmosphere over Electris, so that neither model can apparently be ruled out on this basis. Furthermore, we suggest that such heat budget studies are not sufficiently precise to be used as the overriding basis for choosing atmospheric models. This conclusion should not be surprising considering the present state of the art as it applies to our own atmosphere. There are, after all, still several regions in the terrestrial atmosphere whose heat budgets are poorly understood, not to mention a number of anomalies which also contribute to remaining uncertainties, even though intensive experimental and theoretical work has been carried out over many decades.

The atmospheric data obtained from the Mariner IV occultation experiment have apparently resolved several important immediate problems, but have also raised a large number of more definitive questions. Of prime importance in future occultation measurements would be the ability

to detect lower ionization densities and to study both the neutral and ionized portions of the atmosphere over different topographical areas at different latitudes, times of day, and seasons of the year. The higher sensitivity for ionospheric measurements is needed to help resolve remaining ambiguities in the model studies and in the first-order density and temperature profiles. Improved sensitivity could be provided by a dual frequency experiment (20), and this would also make possible experimental separation of dispersive plasma effects from the non-dispersive refraction of the neutral atmosphere. Repeated measurements at a large number of different locations, times, and seasons are of obvious and critical importance in the atmospheric and ionospheric studies, and in addition would impact on problems related to global Martian weather, the polar caps, topographic and elevation differences between maria and deserts, and the average oblate shape of the planet. The requirement for repeated occultation measurements obviously points to a simple radio-transponder experiment in an orbiter. From the orbital parameters that would be derived as part of this experiment, added information on the mass of Mars and its higher gravitational moments could also be determined.

REFERENCES AND NOTES

1. A. J. Kliore, D. L. Cain, G. S. Levy, V. R. Eshleman, G. Fjeldbo, and F. D. Drake, Science, 140, 1243, (1965). A. J. Kliore, D. L. Cain, F. D. Drake, V. R. Eshleman, G. Fjeldbo, and G. S. Levy, Proc. Caltech-JPL Lunar and Planetary Conf., Pasadena, California, September 13-19, 1965.
2. D. L. Cain, F. D. Drake, V. R. Eshleman, G. Fjeldbo, A. J. Kliore, and G. S. Levy, Proc. Ionospheric Res. Comm. Avionics Panel, Advisory Group for Aerospace Research and Development, NATO, Rome, Italy, September 21-25, 1965.
3. G. Fjeldbo, V. R. Eshleman, A. J. Kliore, D. L. Cain, G. S. Levy, and F. D. Drake, Proc. Caltech-JPL Lunar and Planetary Conf., Pasadena, California, September 13-18, 1965.
4. G. Fjeldbo, W. C. Fjeldbo, and V. R. Eshleman, J. Geophys. Res., 71, 2307, (1966).
5. F. S. Johnson, Science, 150, 1445, (1965).
6. T. M. Donahue, Science, 152, 763, (1966).
7. N. Smith and A. Beutler, "A Model Martian Atmosphere and Ionosphere," Rpt. no. 66-3, Univ. of Michigan Radio Astronomy Observatory, Dept. of Astronomy, Dept. of Electrical Engineering, Ann Arbor, Michigan, March 1966.
8. J. W. Chamberlain and M. B. McElroy, Science, 152, 21, (1966).
9. F. F. Marmo and P. Warwick, "Laboratory and Theoretical Studies in the Vacuum Ultraviolet for the Investigation of the Chemical Physics of Planetary Atmospheres," Contract NASw-124, Quarterly Progress Reports, Geophysical Corporation of America, Bedford, Massachusetts, 3 August 1960 and 3 August 1961.
10. G. Ohring, Icarus, 1, 328, (1963). Similar calculations by C. Prabhakara and J. S. Hogan, Jr. [J. Atmos. Sci., 22, 97, 1965] gave considerably higher stratospheric temperatures.
11. J. W. Chamberlain, Astrophys. J., 136, 582, (1962).
12. P. J. Nawrocki and R. Papa, Atmospheric Processes, Prentice-Hall, New Jersey (1963).
13. D. R. Bates, Proc. Phys. Soc., London B64, 805, (1951); I. Harris and W. Priest, J. Geophys. Res., 67, 4585, (1962); M. B. McElroy, J. L'Ecuyer, and J. W. Chamberlain, Astrophys. J., 141, 1523, (1965); M. Nicolet, Planet Space Sci., 5, 1, (1961).

14. It can be argued that the 24-hour average temperature profile should be lower than the temperatures obtained by solving Eq. (1) because the average solar zenith angle was larger than 67° at Electris on the day of the experiment. The actual temperatures prevailing in the thermosphere at the time of the measurements were, on the other hand, probably somewhat larger than the diurnal average profile so that the temperatures obtained from Eq. (1) might still offer the best basis for comparisons.

We have also studied the steady state temperature profiles for $\chi = 67^\circ$, which presumably represent upper limits to the actual temperatures prevailing in the thermosphere during the occultation experiment. These computations were done by removing the factor "1/2" in front of the solar flux term of Eq. (1). This change increased the thermopause temperatures by approximately 50%.

15. Below 200 Å we used the quiet sunspot minimum solar X-ray intensities given in Table 4-4 in F. S. Johnson's Satellite Environment Handbook, Stanford University Press, 1965 edition. Between 200 and 1000 Å we used data taken from H. E. Hinteregger, L. A. Hall, and G. Schmedtke, "Solar XUV Radiation and Neutral Particles Distribution in July 1963 Thermosphere," Fifth International Space Science Symposium, Florence, Italy, 1964. For longer wavelengths, we used data from Fig. 4-2 of F. S. Johnson's Satellite Environment Handbook.
16. S. H. Gross, W. E. McGovern, and S. I. Rasool, *Science*, 151, 1216, (1966).
17. A. J. Kliore, D. L. Cain, and G. S. Levy, "Radio Occultation Measurement of the Martian Atmosphere over Two Regions by the Mariner IV Space Probe," Presented to the Seventh International Space Science Symposium, Committee on Space Research (COSPAR), Vienna, Austria, May 11-17, 1966.
18. R. B. Leighton and B. C. Murray, "The Behavior of Carbon Dioxide and Other Volatiles on Mars," submitted to Science, April 8, 1966.
19. G. de Vaucouleurs, Physics of the Planet Mars, Faber and Faber, Ltd., London (1954), p. 202.
20. G. Fjeldbo, V. R. Eshleman, O. K. Garriott, and F. L. Smith, III, J. Geophys. Res., 70, 3701, (1965).
21. Research reported herein was supported by NASA grants NGR-05-020-065 and NsG-377.